Proc. Natl. Acad. Sci. USA
Vol. 86, pp. 881–885, February 1989
Biophysics

Inhibition of growth of nonbasal planes in ice by fish antifreezes

(crystal growth inhibition/proteins/adsorption/dislocations/crystal habit)

JAMES A. RAYMOND*†, PETER WILSON‡, AND ARTHUR L. DEVRIES§

*Alaska Department of Fish and Game, 1300 College Road, Fairbanks, AK 99701; †Institute of Marine Science, University of Alaska, Fairbanks, AK 99701; ‡Department of Physics, University of Otago, Dunedin, New Zealand; and §Department of Physiology and Biophysics, University of Illinois, Urbana, IL 61801

Communicated by H. A. Lowenstam, October 17, 1988 (received for review August 19, 1988)

ABSTRACT **Peptide and glycopeptide antifreezes from a variety of cold-water fishes cause ice single crystals grown from the melt to assume unusual and strikingly similar habits. The antifreezes inhibit growth on the prism faces but allow limited growth on the basal plane. As new layers are deposited on the basal plane, pyramidal surfaces develop on the outside of the crystal, and large hexagonal pits form within the basal plane. The pits are rotated 30° with respect to the normal orientation of hexagonal ice crystals. Growth inhibition on the prism, pyramidal, and pit faces indicates that these faces contain sites of adsorption of the antifreeze molecules. Several properties of the antifreeze pits are consistent with (but do not prove) an origin of the pits at dislocations. The similarity of crystal habit imposed on ice by antifreezes with wide differences in composition and structure indicates a common mechanism.**

Fishes inhabiting polar and subpolar marine waters have a variety of peptide and glycopeptide antifreezes that protect them from freezing (1–3). The antifreezes lower the temperature at which an ice crystal will grow but they do not lower the melting point. The activity of the antifreezes has been attributed to inhibition of ice growth through adsorption to the ice surface (4, 5).

Adsorbents often bind to specific faces of crystals; by inhibiting growth on those faces, they can markedly alter crystal habit. Several of the antifreezes, for example, cause ice to grow in the shape of needles aligned with the *c* axis when the temperature is lowered below the freezing point (4, 6). Because ice normally grows most rapidly in directions perpendicular to the *c* axis (7), it is clear that the antifreezes inhibit growth in these directions. However, few other details are known about the adsorption process. A better understanding of the antifreeze adsorption may also provide insights into the mechanisms of other proteins that (*i*) inhibit the growth of biocrystals, such as bone minerals (8, 9), enamel (10), cholesterol crystals (11), and kidney stones (12); and (*ii*) act as crystal nucleators (13, 14), since the processes of nucleation and growth inhibition are closely related (13). To learn more about the effects of the antifreezes on ice crystal habit, and thus the manner in which they bind to ice, the freezing behavior of ice single crystals was observed in the presence of aqueous solutions of six antifreezes (Table 1).

The antifreezes differ widely in their compositions and structures. The antifreeze of *Dissostichus mawsoni* is a series of eight glycopeptides ranging in molecular mass from 2400 to 34,000 Da (2). The larger fractions (gp1–5) have a greater freezing point depressing activity than the smaller fractions (gp6–8). The basic structure is a repeating tripeptide-disaccharide unit in an extended coil configuration. The presence of 3-fold helical segments has been suggested (15). The other antifreezes consist only of peptide chains. The antifreezes of the zoarcids [*Rhigophila dearborni* (6), *Macrozoarces americanus*¶ (16), and *Austrolycicthys brachycephalus* (A.L.D., unpublished data)] are roughly similar. The amino acid sequences have between 61 and 64 residues, are nonrepeating, and have homologies ranging from 56% to 69%. The *Macrozoarces* antifreeze appears to have a distinct tertiary structure that lacks both α-helical and β-components. The antifreeze of *Hemitripteris americanus* (3) has a molecular mass of 17,000 Da and a nonrepeating sequence that differs from the zoarcid sequences. Its secondary structure includes both β- and α-helical components. The antifreeze of *Myoxocephalus scorpius* (17) is present in two fractions of 4000 and 2900 Da. Both fractions contain an 11-amino acid repeating sequence with a high alanine content and have conformations that are largely α-helical. The helical portion of the larger fraction appears to be amphiphilic—i.e., all of the polar residues appear to be on one side of the helix.

Table 1. Fishes from which antifreezes were obtained for this study

Species	Family	Distribution
D. mawsoni	Nototheniidae	Antarctic
R. dearborni	Zoarcidae	Antarctic
M. americanus	Zoarcidae	North Atlantic
A. brachycephalus	Zoarcidae	Antarctic
H. americanus	Cottidae	North Atlantic
M. scorpius	Cottidae	North Atlantic

MATERIALS AND METHODS

The glycopeptide antifreezes were isolated from blood serum by DEAE ion-exchange chromatography (18). Peptide antifreezes were isolated with G-75 Sephadex gel filtration followed by reverse-phase HPLC (6).

Single crystals of ice were grown from deionized water in a 2-liter insulated container in a −2°C cold room. Under conditions of slow growth such as these, ice crystals are known to develop facets (19, p. 54). Within 2 days, crystals in the shape of elongated plates grew to a size of ≈4 mm wide and ≈1 mm thick (Fig. 1*A*). The ends of the plates were sharply defined, giving the plates a hexagonal appearance. The edges of the crystals were assumed to be first-order prism faces (the $\{10\bar{1}0\}$ faces) because these faces are known to develop when ice crystals are grown from the vapor (20). To confirm this, a vapor-grown hexagonal ice crystal obtained from an ice cave was used on one occasion. The orientation of hexagonal pits (described below) that formed on this crystal in the presence of the antifreezes was the same as that found on crystals grown from the melt. Crystals were cut to a length of ≈6 mm. The cut edge was usually parallel to a second-order prism face, while the remaining four edges were first-order prism faces. One of the basal planes of a crystal was frozen to a glass slide.

The publication costs of this article were defrayed in part by page charge payment. This article must therefore be hereby marked "*advertisement*" in accordance with 18 U.S.C. §1734 solely to indicate this fact.

¶The amino acid sequence of an antifreeze precursor was reported. Residues 23–84 of that precursor, which resembled the sequences of the other zoarcid antifreezes, was used for this comparison.

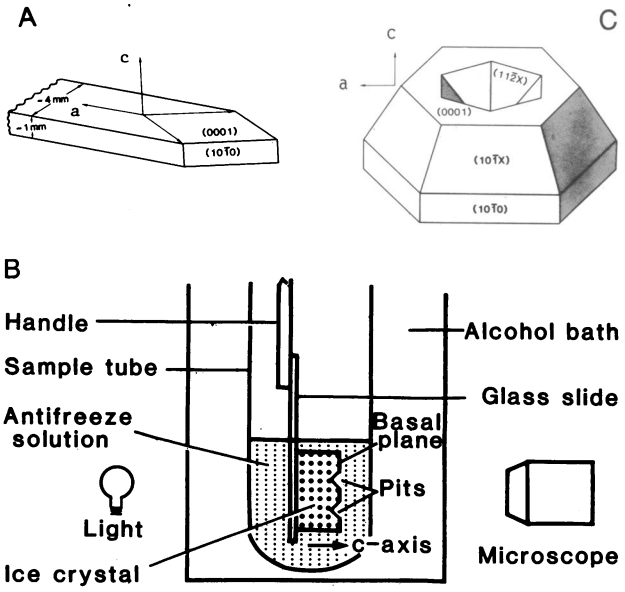

FIG. 1. Schematic drawings of ice crystals. (*A*) Faceted ice crystal grown slowly in pure water. (*B*) Experimental apparatus used to observe growth of ice single crystals in the presence of fish antifreezes. (*C*) Ice crystal showing major faces developed in the presence of fish antifreezes.

The experimental apparatus used for observing the growth of ice crystals in the presence of the antifreezes is shown in Fig. 1*B*. Approximately 1.0 ml of an aqueous solution of antifreeze was placed in a 1-cm-diameter glass tube. The tube was placed in a temperature bath with rear and front windows and equilibrated at approximately −0.1°C. A proportional temperature controller maintained temperatures to within 0.01°C. The ice crystal, mounted on the slide, was equilibrated at approximately −0.1°C and then placed in the antifreeze solution. Ice crystals were viewed and photographed with a horizontal ordinary light microscope.

Observations were made at temperatures between the melting point and "freezing point" of the antifreeze solution. The freezing point is not a true equilibrium freezing point but the temperature at which rapid growth of a polycrystalline seed crystal occurs. At temperatures between the melting point and freezing point, neither melting nor bulk freezing occurs. Subtle changes in single crystals can thereby be observed. Antifreeze concentrations were usually between 5 and 10 mg/ml. At these concentrations, the melting point is approximately −0.02°C and the freezing point is typically −0.7 to −1.0°C.

Refraction patterns were created by directing a helium-neon laser beam through the temperature bath windows. The incident beam was normal to the bath windows and parallel to the *c* axis of the ice crystal. The incident beam passed through the unpitted side of the crystal and emerged on the pitted side. The beam was refracted twice: once by the ice–antifreeze solution interface on the pit faces and again by the equivalent of an antifreeze solution–air interface. In all cases, the orientation of the refraction spots about the *c* axis was the same as that of the faces on the pits. The slope of the refracting surfaces on the ice crystal was calculated from the angle of the refracted beams.

RESULTS

The antifreezes, in view of their differences in composition and structure, showed striking similarities in their effects on the crystal habit of ice. With one exception, each of the antifreezes inhibited the growth of the prism faces (the faces parallel to the *c* axis) of a single crystal. In addition, all of the antifreezes completely halted growth of the ice crystal after allowing limited growth on the basal plane. During the growth phase, two changes in crystal habit occurred: pyramidal faces developed on the exterior of the crystal and hexagonal pits developed within the basal plane. These features are shown schematically in Fig. 1*C*. Pyramidal faces originating from the first-order prism faces [the {10$\bar{1}$0} faces] were usually of the form {10$\bar{1}$X}, while those originating from the second-order prism faces [the {11$\bar{2}$0} faces] were usually of the form {11$\bar{2}$X′}. The pits grew in size not by the removal of material, but by the addition of new layers to the basal plane. Pit diameters often reached several hundred micrometers. An unusual feature of the pits was their orientation: the pit edges were rotated 30° with respect to the first-order prism faces of the crystals, producing pit faces of the form {11$\bar{2}$X″}.

Glycopeptide Antifreezes. The major effects of the antifreezes on the growth of ice are demonstrated by the glycopeptide antifreezes. gp1–5, the most active fraction, completely halted growth on the prism faces but allowed limited growth on the basal plane. Fig. 2*A* shows an ice single crystal immersed in a solution of gp1–5 at −0.04°C. A basal plane containing a few pits is shown at the bottom and a pyramidal face is shown at the top. Fig. 2*B* shows the crystal 37 min later. The crystal grew ≈400 μm in a direction parallel to the *c* axis, which resulted in the enlargement of existing pits and the formation of new pits. No growth could be detected on either the pit faces or the pyramidal face shown in Fig. 2*A*. Another photograph taken 74 min after that shown in Fig. 2*B* showed no further changes in the crystal. Measurements of the photographs show that the growth velocity parallel to the *c* axis was $\approx 1.7 \times 10^{-5}$ cm·s^{-1}. This value is comparable to values reported for *c* axis growth at the same temperature in the absence of growth inhibitors (21).

Growth of the crystal was limited to the basal plane, which, because of the growth of pits and pyramidal faces, gradually decreased in area. When no growth areas remained on the basal plane, growth stopped. At low supercoolings, a few unpitted islands, like the one shown in Fig. 2*B*, usually remained on the basal plane.

Pits grown in the presence of gp1–5 at low supercoolings ranged in size from 100 to 600 μm in diameter and had a density on the order of 10^3 cm^{-2}. Higher supercoolings produced more rapid growth on the basal plane and smaller pits. Antifreeze concentrations between 0.5 and 20 mg/ml did not noticeably affect the diameter of the pits. Even at very

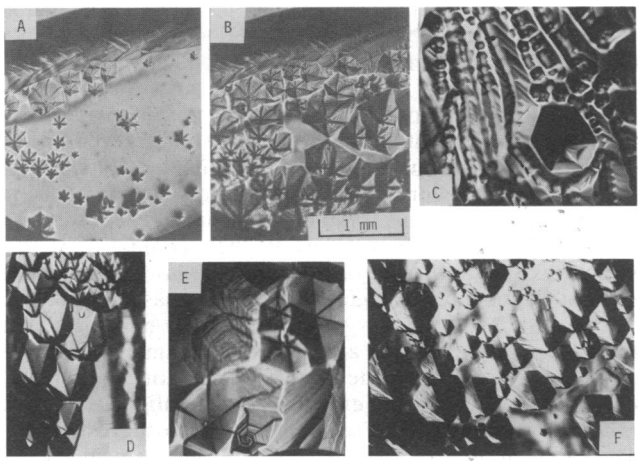

FIG. 2. Photographs of pits grown in ice crystals in the presence of antifreezes from various fishes, viewed at an angle from above the basal plane. All photographs are in the same scale as shown in *B*. (*A* and *B*) *Dissostichus* (see text). (*C*) *Macrozoarces*. (*D*) *Rhigophila*. (*E*) *Hemitripteris*. (*F*) *Myoxocephalus*.

low concentrations (25 and 2.5 μg/ml), pits with the same orientation formed. However, their density was low.

Ice single crystals grown in the presence of a 10 mg/ml solution of gp7 and -8 at approximately −0.05°C grew in a direction parallel to the *c* axis. Pits did not form but hexagonal pyramidal surfaces of the form {10$\bar{1}$X} developed (Fig. 3*A*). Unlike the other antifreezes, gp7 and -8 allowed growth on both first- and second-order prism faces, so that each such face "filled out" until only {10$\bar{1}$X} surfaces remained. This resulted in the growth of complete hexagonal pyramids. Once the pyramid was completed, no further growth occurred. Similar pyramidal growth, without pitting, occurred at concentrations of 20 and 40 mg/ml.

gp6 showed some of the properties of both gp1–5 and gp7 and -8. This intermediate-sized fraction prevented growth on the prism faces and caused many small pits to grow on the basal plane. However, continued growth on the pit faces caused the crystal to eventually assume a pyramidal shape.

Peptide Antifreezes. In the presence of the peptide antifreezes, no growth was observed on either first- or second-order prism faces of ice single crystals or on the pyramidal surfaces that developed during growth on the basal plane. Pits that formed in the basal plane (Fig. 2 *C–F*) had the same orientation and approximately the same size range as those grown with gp1–5. In all cases, after limited growth in the *c* axis direction, growth of the crystals came to a complete halt.

Although the major effects of the peptide and glycopeptide antifreezes on ice were the same, the peptide antifreezes, like gp6, were not as effective as gp1–5 in halting growth on the pit faces. The pits initially formed with smooth faces, a feature that was demonstrated by sharp refraction patterns (Fig. 4 *b* and *c*). However, growth on the pit faces continued, causing the faces to become stepped, irregular, and more steeply sloped. In the presence of the *Rhigophila* and *Myoxocephalus* antifreezes, growth stopped after the pits reached a depth of ≈1 mm. With the other three peptide antifreezes, growth continued until a complete pyramid was formed. Fig. 3*B* shows such a pyramid midway in its growth.

Spiral steps appeared to be the points of growth in the presence of the *Hemitripteris* antifreeze (Fig. 2*E*). Rows of pits, which were observed to form in the presence of the *Macrozoarces* (Fig. 2*C*) and *Rhigophila* antifreezes and also gp6, appeared to be aligned in directions both parallel and perpendicular to the *a* axis. These features may be associated with dislocations in ice (see *Discussion*).

Adsorption Planes. Identification of the pit and pyramidal faces on the ice crystals is of interest because the arrangement of hydrogen and oxygen atoms on these faces is presumably responsible for the antifreeze adsorption. At low magnification, pits grown in the presence of gp1–5 appeared to have six faces. At higher magnification, the hexagonal faces were usually found to consist of two faces at a slight angle to one another (Fig. 5*A*). A refraction pattern of the pits is shown in Fig. 4*A*. The angle of the brightest portion of the refracted beams, 2.8°, indicated that the slope of the pit faces was ≈60°. This slope and the orientation of the pits suggest that the (12 sided) pit faces are of the form {n, $n+1$, $\overline{2n+1}$, $2n+1$} (n = 1, 2 ...).‖ In this model, the lines between the bottom of a pit and the centers of the hexagonal faces are the ⟨11$\bar{2}$2⟩ directions, regardless of the value of n. The ⟨11$\bar{2}$2⟩ directions thus lie on the 12-sided pit faces. Pits with {23$\bar{5}$5} faces (n = 2) have angles on the upper edges that appear to most closely resemble those in the photographs. A stereo view of this model pit is shown in Fig. 5*B*.

Slopes of other pit faces and the pyramidal faces generally differed from those of low-index planes (Table 2) and are thus difficult to identify. Variations in slope were also observed: several pyramids grown with gp7 and -8 each had slightly different slopes and, as previously stated, pit faces that formed in the presence of the peptide antifreezes changed slope during the growth phase. These observations suggest that, in general, the {10$\bar{1}$X} pyramid surfaces and the {11$\bar{2}$X} pit surfaces were composed of steps that were too small to resolve at ×40 magnification. A possible exception was the pyramidal faces formed in the presence of *Hemitripteris* antifreeze. The slope of these faces was close to that of the {10$\bar{1}$1} planes.

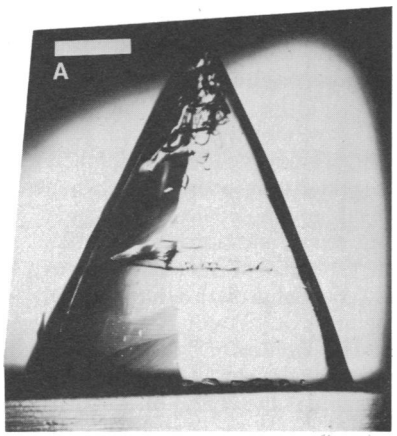

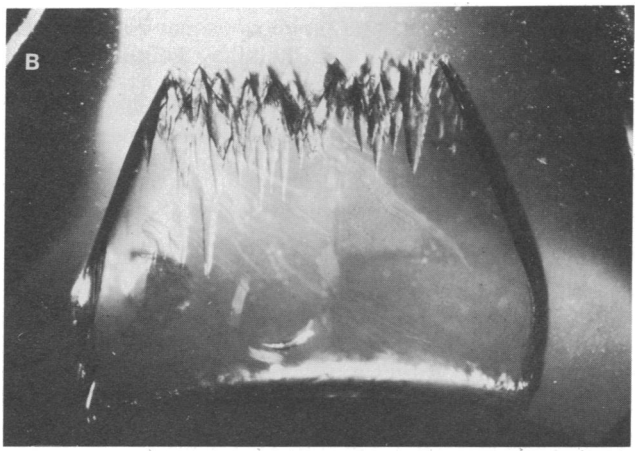

FIG. 3. Hexagonal pyramidal ice crystals grown with two antifreezes. The *c* axis is vertical and the *a* axis is normal to the page. (*A*) *Dissostichus* gp7 and -8. (*B*) *Austrolycicthys*. The crystal is shown while it was still growing. Pitting is visible on the basal plane. (Bar = 1 mm.)

DISCUSSION

Many cases of crystal growth inhibition by adsorbed impurities have been reported (13, 22, 23). In almost all cases, growth inhibition was accompanied by changes in crystal habit. The development of different crystal faces in the presence of an impurity is thought to be due to a preferential affinity of the impurity for those faces (24). As each new layer is deposited on an adjacent faster-growing face, the retarded face increases slightly in area. The result is a crystal whose habit is dominated by its slowest-growing faces. Because ice crystal habit is normally dominated by basal planes, the nonbasal planes that develop in the presence of the antifreezes are thus a strong indication that they are sites of antifreeze adsorption. In contrast, adsorption to the basal plane appears to be minimal or nonexistent. The effectiveness of the antifreezes as adsorbents is shown by their ability

‖As n becomes large, the angle between the two faces of a double-sided face approaches zero and the pit becomes a six-sided pyramid with {11$\bar{2}$2} faces.

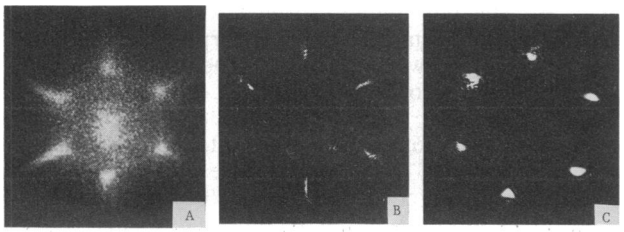

FIG. 4. Refraction spots produced by directing a laser beam through an ice crystal pitted by different antifreezes. Path of incident beam was parallel to the *c* axis. (*A*) *Dissostichus* (gp1–5). Refracted beams from each half of a double-sided face appear too close to resolve. The central spot is due to light transmitted through unpitted portions of the basal plane. (*B*) *Rhigophila*. (*C*) *Hemitripteris*.

to completely halt the growth of ice after allowing limited growth on the basal plane.

The development of similar faces in ice by the antifreezes, despite considerable differences in their compositions and structures, indicates that the antifreezes have similar affinities for ice. What properties might they have in common to account for this? One such property may be lattice matching in which the spacing between adjacent polar groups on an antifreeze peptide matches the spacing between various oxygen and hydrogen atoms in the ice lattice. This would promote hydrogen bonding between the antifreeze and the ice (1). Similar lattice matching models have been proposed for other proteins that act as nucleators of ice (14) and certain calcium salts (13). A similar spacing between polar groups on different antifreezes could result in affinities for the same crystal planes and thus could account for the similarities in crystal habit. It should be noted that proper orientation of

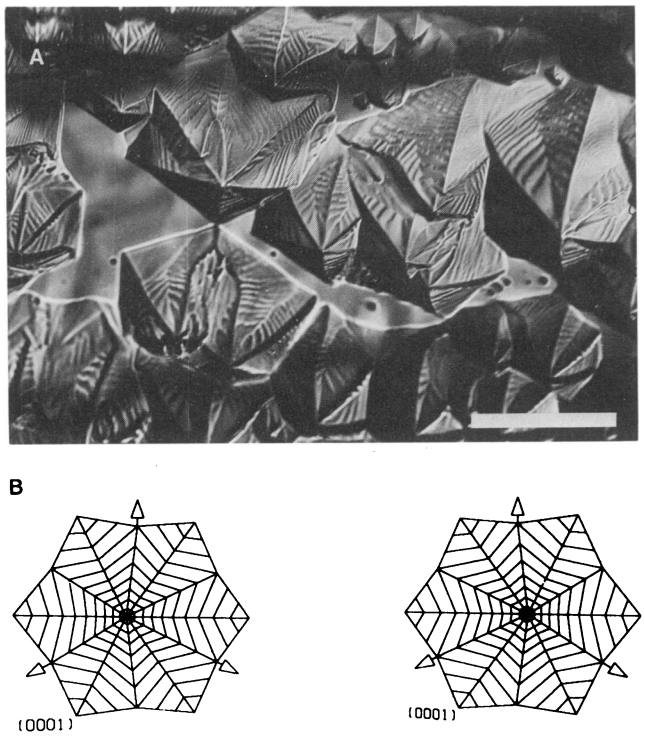

FIG. 5. Pits grown in the presence of gp1–5. (*A*) Detail of Fig. 2*B*. The basal plane appears as a flat area surrounded by pits. The pits are mostly double-sided with chevron-like steps. A pit face with a single-sided upper portion is shown at left and below center. (*B*) Stereo pair of a model pit using $\{23\bar{3}5\}$ faces. Arrows point in directions of *a* axes. In this model, the directions that most closely resemble the step fronts in the photographs are the $\langle 5\ 5\ \bar{1}0\ 6\rangle$ directions; several such steps are shown. (Bar = 1 mm.)

Table 2. Approximate slopes (in degrees) of pyramidal and pit faces grown in the presence of fish antifreezes (slopes of low-index planes are included for comparison)

Pyramidal faces $\{10\bar{1}X\}$		Pit faces $\{11\bar{2}X\}$	
Antifreeze	Slope	Antifreeze	Slope
$\{10\bar{1}1\}$	62.1	$\{11\bar{2}2\}$	58.5
Dissostichus (gp6)	72	*Rhigophila*	66.8
Dissostichus (gp7 and -8)	65–73	*Hemitripteris*	54.8
Austrolycicthys	68		
Hemitripteris	61.5		

Slopes of pyramidal faces were obtained from photographs and direct measurement of crystals; slopes of pit faces were obtained from refraction patterns.

reactive groups on the crystal face, as well as their spacing, may be required for binding to occur (13).

Recently, Yang *et al.* (25) discounted the importance of lattice matching in the binding to ice of an α-helical antifreeze that is roughly similar to that of *M. scorpius*. From the molecule's crystal structure, they concluded that the helix was a dipole and that the hydrophilic side chains had multiple conformations, thus reducing its specificity. Yang *et al.* proposed that the helix dipoles induce local ice dipoles on the prism faces and are subsequently attracted to them. Hydrogen bonding between the antifreeze and ice was assumed to occur after alignment of the helix and ice dipoles. This hypothesis is consistent with inhibition of growth on the prism faces described here. However, all but one of the antifreezes used in this study differed considerably from the α-helical antifreeze used by Yang *et al.*

Another possible common property is amphiphilicity, in which polar groups on the hydrophilic side of the antifreeze adsorb to the ice lattice and nonpolar groups on the hydrophobic side deter other water molecules from joining the ice lattice. Presently, evidence for amphiphilicity has been found only for the peptide antifreezes having α-helical structures (1, 17). In principal, any molecule that has a crystal-loving side and a side that repels additions to the crystal can be used to inhibit crystal growth. This idea has been exploited to create "tailor-made" crystal growth inhibitors (26).

Binding of antifreezes along a single crystal direction, either by lattice matching or by a dipole–dipole interaction, can account for the development of several different crystal faces. An example is the $\langle 11\bar{2}2\rangle$ directions. These directions lie on the $\{10\bar{1}0\}$ prism faces, and, if the model described above is correct, on the 12-sided pit faces formed in the presence of gp1–5. The $\langle 11\bar{2}2\rangle$ directions may also lie on the pyramidal surfaces, provided that they consist of $\{10\bar{1}0\}$ steps, and on the faces of *c* axis ice needles that form when many antifreeze solutions are frozen, provided that the needles are bounded by $\{10\bar{1}0\}$ faces. It should be noted that gp7 and -8, despite their similarity in composition to gp1–5, appear to differ in their type of binding to ice, since these low molecular weight antifreezes fail to form pits, even at high concentrations.

The occasional appearance of stable unpitted islands on the basal plane in the presence of gp1–5 indicates that under low supercoolings, this antifreeze is capable of blocking growth on the basal plane. A recent report suggested that gp1–5 block growth in the *c* axis direction by inhibiting surface nucleation on the basal plane (27). Although our present results show that this is not the major mechanism by which the antifreezes stop growth in the *c* axis direction, such a mechanism might be capable of producing nongrowing portions on the basal plane. Growth normally occurs at steps that are created by dislocations in the crystal lattice. In small areas of the basal plane that are free of dislocations, inhibition of surface nucleation could prevent further growth. One way in which

gpl–5 could inhibit surface nucleation is through lattice strain, which has been suggested as a mechanism of inhibition of surface nucleation in certain protein crystals (28). Because gpl–5 are incorporated into ice during freezing (4), it is possible that the lattice is distorted to some degree in the vicinity of the adsorbed antifreeze molecules, thus inhibiting the formation of nuclei.

The antifreeze pits superficially resemble etch pits that form at dislocation sites on the basal plane in the presence of solutions of Formvar (29–31). Unlike the antifreeze pits, however, the etch pits are formed by the removal of material from the ice, have edges that are parallel to the *a* axes (32), and are relatively shallow. Despite these differences, several characteristics of the antifreeze pits suggest a link between them and dislocations. These include growth spirals and rows of pits, which, when found in etched surfaces, have been attributed to stationary (33–35) and gliding (36–38) screw dislocations, respectively. Furthermore, the direction of the rows of antifreeze pits are the same as those found in the rows of etch pits. As stated above, there is also the possibility that unpitted areas on the basal plane in the presence of gpl–5 are due to an absence of dislocations. The increase in density of pits that occurred with gpl–5 at higher supercoolings is also consistent with a dislocation origin of the pits, since rapid freezing causes a greater density of dislocations (39). Recently, Shimon *et al.* (26) have shown by the etching of various organic crystals that a strong relation exists between dislocations and sites of adsorption by impurities. Further studies are needed to determine what role, if any, dislocations play in the adsorption of the antifreezes to ice.

We thank Drs. Charles Knight and N. K. Sinha for valuable discussions. Helpful comments on the manuscript were provided by Chris DeVries. This work was supported in part by National Science Foundation Grant DPP87-16296 to A.L.D. Support by the Japanese National Institute for Polar Research to J.A.R. is gratefully acknowledged.

1. DeVries, A. L. (1982) *Comp. Biochem. Physiol. A* **73,** 627–640.
2. DeVries, A. L. (1983) *Annu. Rev. Physiol.* **45,** 245–260.
3. Ng, N. F., Trinh, K. & Hew, C. L. (1986) *J. Biol. Chem.* **261,** 15690–15695.
4. Raymond, J. A. & DeVries, A. L. (1977) *Proc. Natl. Acad. Sci. USA* **74,** 2589–2593.
5. DeVries, A. L. (1984) *Philos. Trans. R. Soc. London Ser. B* **304,** 575–588.
6. Schrag, J. D., Cheng, C. C., Panico, M., Morris, H. R. & DeVries, A. L. (1987) *Biochim. Biophys. Acta* **915,** 357–370.
7. Fletcher, N. H. (1970) *The Chemical Physics of Ice* (Cambridge Univ. Press, Cambridge).
8. Price, P. A., Otsuka, A. S., Poser, J. W., Kristaponis, J. & Raman, N. (1976) *Proc. Natl. Acad. Sci. USA* **73,** 1447–1451.
9. Blumenthal, N. C., Betts, F. & Posner, A. S. (1975) *Calcif. Tissue Res.* **18,** 81–90.
10. Aoba, T., Fukae, M., Tanabe, T., Shimizu, M. & Moreno, E. C. (1987) *Calcif. Tissue Int.* **41,** 281–289.
11. Kibe, A., Holzbach, R. T., LaRusso, N. F. & Mao, S. J. T. (1984) *Science* **225,** 514–516.
12. Nakagawa, Y., Abram, V., Kezdy, F. J., Kaiser, E. T. & Coe, F. L. (1983) *J. Biol. Chem.* **258,** 12594–12600.
13. Addadi, L. & Weiner, S. (1985) *Proc. Natl. Acad. Sci. USA* **82,** 4110–4114.
14. Warren, G. J. & Wolber, P. K. (1987) *Cryo-Letters* **8,** 204–215.
15. Feeney, R. E., Burcham, T. S. & Yeh, Y. (1986) *Annu. Rev. Biophys. Chem.* **15,** 59–78.
16. Li, X.-M., Trinh, K.-Y., Hew, C. L., Buettner, B., Baenziger, J. & Davies, P. L. (1985) *J. Biol. Chem.* **260,** 12904–12909.
17. Hew, C. L., Joshi, S., Wang, N.-C., Kao, M.-H., Anantharayanan, V. S. (1985) *Eur. J. Biochem.* **151,** 167–172.
18. DeVries, A. L., Komatsu, S. K. & Feeney, R. E. (1970) *J. Biol. Chem.* **245,** 2901–2908.
19. Luyet, B. & Rapatz, G. (1958) *Biodynamica* **8,** 22–68.
20. Higuchi, K. & Yosida, T. (1967) in *Physics of Snow and Ice*, ed. Oura, H. (Institute of Low Temperature Science, Hokkaido Univ., Sapporo, Japan), Vol. 1, pp. 79–93.
21. Hillig, W. (1958) in *Growth and Perfection of Crystals*, ed. Doremus, R. H. (Wiley, New York), pp. 350–360.
22. Raymond, J. A. (1976) Thesis (Univ. of Calif., San Diego).
23. Berman, A., Addadi, L. & Weiner, S. (1988) *Nature (London)* **331,** 546.
24. Buckley, H. E. (1952) *Crystal Growth* (Wiley, New York).
25. Yang, D. S. C., Sax, M., Chakrabartty, A. & Hew, C. L. (1988) *Nature (London)* **333,** 232.
26. Shimon, L. J. W., Lahav, M. & Leiserowitz, L. (1986) *N. J. Chem.* **10,** 723.
27. Harrison, K., Hallet, J., Burcham, T. S., Feeney, R. E., Kerr, W. L. & Yeh, Y. (1987) *Nature (London)* **328,** 241–243.
28. Davey, R. J. (1986) *J. Cryst. Growth* **76,** 637–644.
29. Sinha, N. K. (1977) *Philos. Mag.* **36,** 1385–1404.
30. Truby, F. K. (1955) *J. Appl. Phys.* **26,** 1416–1420.
31. Kuroiwa, D. & Hamilton, W. L. (1963) in *Ice and Snow*, ed. Kingery, W. D. (MIT Press, Cambridge, MA), pp. 34–55.
32. Higuchi, K. (1958) *Acta Metallurgica* **6,** 636–642.
33. Bryant, G. W. & Mason, B. J. (1960) *Philos. Mag.* **5,** 1221–1227.
34. Muguruma, J. (1961) *Nature (London)* **190,** 37–38.
35. Muguruma, J. (1963) *Nature (London)* **208,** 180–181.
36. Muguruma, J. & Higashi, A. (1963) *Nature (London)* **198,** 573.
37. Levi, L., de Achaval, E. M. & Suraski, E. (1965) *J. Glaciol.* **5,** 691–699.
38. Unwin, P. N. T. & Muguruma, J. (1971) *Appl. Phys.* **42,** 3640–3641.
39. Higashi, A. & Oguro, M. (1967) *Ohyo-Butsuri (Appl. Phys.)* **36,** 988–994.